Cobalt(III) and copper(II) hydrides at the crossroad of catalysed chain transfer and catalysed radical termination: a DFT study

S. M. Wahidur Rahaman, K. Matyjaszewski, Rinaldo Poli

Polymer Chemistry

ARTICLE

Cobalt(III) and copper(II) hydrides at the crossroad of catalysed chain transfer and catalysed radical termination: a DFT study

Received 00th January 20xx,
Accepted 00th January 20xx

DOI: 10.1039/x0xx00000x

www.rsc.org/

S. M. Wahidur Rahaman,[a] Krzysztof Matyjaszewski [b] and Rinaldo Poli*[a,c]

Metal complexes that mediate radical polymerisation may also lead to chain transfer catalysis (CCT) or to catalysed radical termination (CRT), both processes occurring via the same type of hydride intermediate. What leads these intermediates to prefer reacting with monomer, leading to CCT, or with radicals, leading to CRT, was unclear. We report here a DFT investigation of the comparative reactivity of two different hydride complexes, [(TMP)Co^{III}(H)] (TMP = tetramesitylporphyrin) and [(TPMA)Cu^{II}(H)]$^+$ (TPMA = tris(2-pyridylmethyl)amine), generated from [Co^{II}(TMP)] and [Cu^{I}(TPMA)]$^+$, versus monomer and radical, using the $^{\bullet}CH(CH_3)(COOCH_3)$ and $^{\bullet}C(CH_3)_2(COOCH_3)$ radicals as models for the growing PMA and PMMA radical chains. The unsubstituted porphyrin was used as model for full quantum mechanical (QM) calculations, but selected calculations on the full TMP system were also carried out by the hybrid QM/MM approach, treating the mesityl substituents at the molecular mechanics (MM) level. The calculations provide a basis for rationalizing the experimentally observed strong activity of the cobalt system in catalytic chain transfer (CCT) polymerization without a reported activity so far for catalysed radical termination (CRT), whereas the copper system leads to CRT but does not promote CCT. In essence, the key factors in favour of CCT for the cobalt system are a very low barrier for H transfer to monomer and the much greater concentration of monomer relative to radical, yielding $v_{CCT} > v_{CRT}$. For the copper system, on the other hand, the greater barrier for H transfer to monomer renders the CCT rate much slower, while the CRT quenching pathway favourably takes place through an electronically barrierless pathway with incipient stabilization at long C···H distances. The different spin state of the two systems (spin quenching along the CCT pathway for the Co system and along the CRT pathway for the Cu system) rationalizes the observed behavior. The new acquired understanding should help design more efficient systems.

Introduction

Reversible deactivation radical polymerization (RDRP),[1] in which metal mediated methods occupy a prominent place, is now dominating macromolecular engineering.[2] In ATRP, which is the dominant method within this area,[3-7] the active radical ($P_n^{\bullet}$) concentration is controlled by a dynamic equilibrium (Scheme 1) where an atom (typically a halogen, Y) is transferred to the radical from a suitable metal complex Y-Mt^{x+1}/L, generating a halogen-capped dormant chain P_n-Y and a reduced metal complex Mt^x/L.

Although mechanistically simple, this process may however be accompanied by a number of side reactions[5, 8] that could negatively affect the polymerization control, in some cases even driving the system toward complete failure.[9-11] Most of these side reactions involve the direct interaction of the active radicals with the reduced metal complex. There are three important ways in which a metal complex can react with radicals, as shown in Scheme 2. The first one is to form a direct metal carbon bond, *i.e.* an organometallic dormant species P_n-Mt^{x+1}/L. If this process is reversible and not contaminated by other phenomena, it constitutes an alternative mechanism to control the polymerization (organometallic-mediated radical polymerization, OMRP).[9-14] The second possibility involves an electron transfer and reduction ((or oxidation) of a radical to carbanion (or carbocation) and associated side reactions.[15-17] Another way in which the same two partners can interact is by transfer of a β-H atom to yield the hydride complex H-Mt^{x+1}/L and a dead chain with an unsaturated chain end, $P_n^{(-H)}$. When this occurs, the hydride complex may be able to subsequently transfer the H atom back to a monomer, completing a catalysed chain transfer (CCT) cycle. Cobalt(II) complexes are currently the most efficient catalysts for CCT.[18] An alternative way to obtain the same hydride intermediate is by β-H elimination from the

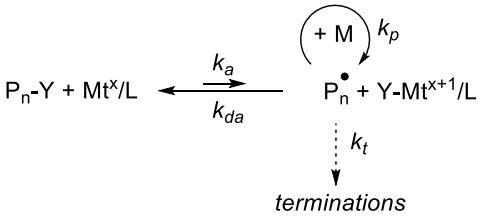

Scheme 1. ATRP controlling mechanism.

[a] *CNRS, LCC (Laboratoire de Chimie de Coordination), Université de Toulouse, UPS, INPT, 205 Route de Narbonne, BP 44099, F-31077, Toulouse Cedex 4, France.*
[b] *Department of Chemistry, Carnegie Mellon University, 4400 Fifth Avenue, Pittsburgh, Pennsylvania 15213, USA.*
[c] *Institut Universitaire de France, 103, bd Saint-Michel, 75005, Paris, France.*
Electronic Supplementary Information (ESI) available: computational details, full table of Cartesian coordinates, energies and views of all optimized geometries. See DOI: 10.1039/x0xx00000x

organometallic dormant chain, a well-known process for certain metals able to catalyse coordination polymerization.[19]

The hydride intermediate H-Mt^{x+1}/L and the organometallic dormant chain P_n-Mt^{x+1}/L, however, may also interact with a new radical chain ($P_m^{\bullet}$). The former leads, through either an H atom transfer process (P_m···H···Mt/L transition state) or an addition/elimination process (via a $Mt^{x+2}(H)(P_m)$/L intermediate) to a dead chain with a saturated chain end $P_m^{(H)}$, regenerating the reduced complex. The latter leads, by a similar process, to a coupled dead chain P_n-P_m. In addition, associative radical exchange processes involving the organometallic dormant species are responsible for controlled radical polymerization by degenerative transfer.[20-22] The two processes leading from H-Mt^{x+1}/L or P_n-Mt^{x+1}/L to dead chains ($P_m^{(H)}$+$P_n^{(-H)}$ or P_n-P_m) and regenerating Mt^x/L constitute catalysed radical terminations (CRT). The CRT phenomenon has recently been discovered as a side reaction in Cu-catalysed ATRP and takes place extensively also when radicals are generated from a conventional initiator (OMRP conditions) rather than from an organic halide (ATRP conditions).[23, 24] It has also been later shown to play a role in Fe-catalysed ATRP.[25] The current evidence is in favour of the hydride complex, rather than the organometallic dormant species, being the key intermediate for CRT. This is shown by the dominant formation of $P_n^{(-H)}$ + $P_m^{(H)}$ dead chains (resembling disproportionation) in Cu-CRT for methyl acrylate,[24] whereas polyacrylates have a natural preference to terminate by coupling in free radical polymerization.[26]

The above described results show that the hydride complex H-Mt^{x+1}/L lies at the crossroad of the CCT and CRT catalytic cycles. While the operating conditions (monomer and metal concentrations, radical flux) are similar, the hydride intermediate H-Co^{III}/L generated by an initiator/Co^{II} system prefers to react with monomer, leading to CCT, whereas the hydride intermediate H-Cu^{II}/L generated by an initiator/Cu^{I} system (or the H-Fe^{III}/L intermediate generated by an initiator/Fe^{II} system) prefers to react with radicals, leading to CRT. To the best of our knowledge, no Cu-CCT process has ever been reported whereas the CRT process has so far not been evidenced in the presence of cobalt complexes. This surprising dichotomy has stimulated us to carry out DFT calculations in an attempt to rationalize the different behaviour of the two metal systems. The goal of the present study is to better understand what factors promote CRT and whether it is possible to engineer system where this phenomenon is suppressed or eliminated, thus improving the ATRP performance. Suppression of CRT may also allow to improve the performance of OMRP systems.

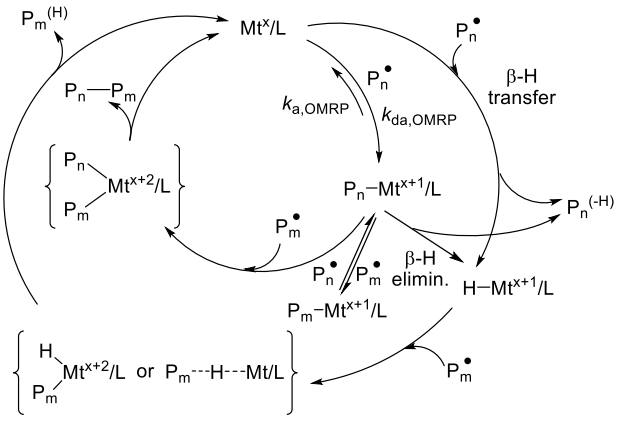

Scheme 2. Possible interactions between an active radical and a reduced metal complex.

Results

(a) Systems and methods selected for the investigation

Comparative calculations of OMRP equilibrium, CCT and CRT energy profiles were carried out for two systems, one based on cobalt(II) and the other one based on copper(I). The three processes are intertwined as illustrated in Scheme 3, which is a simplified version of Scheme 2. On the left, the reversible radical trapping by Mt^x/L leads to the organometallic dormant species. The competitive β-H atom transfer process involving the same two partners (middle) generates the key hydride intermediate H-Mt^{x+1}/L and olefin. The reverse H atom transfer from the hydride complex to the olefin completes the CCT process. On the right, the hydride complex transfers the H atom to a radical to complete the CRT process. The generation of the hydride complex by β-H elimination from the OMRP dormant species has not been considered because this typically occurs for organometallic complexes that can offer a *cis* open coordination site and that are able to bind the produced olefin.[19] This is not the case for the systems of interest here. It is also pertinent to mention that a β-H elimination from an OMRP dormant species was proposed to be responsible for CCT in a Fe^{II}-catalysed ATRP or styrene,[27, 28] but subsequent computational work has indicated that the preferred pathway to CCT is in fact the direct β-H atom transfer from the radical chain to the Fe^{II} catalyst.[29] Finally, on the basis of the evidence discussed in the introduction, the possible CRT via the OMRP dormant species has not been considered in the present investigation. For this process to occur, it would be necessary that the dialkyl intermediate $Mt^{x+2}(P_n)(P_m)$/L has the two chains placed in cis positions and this is certainly not possible, at least for the cobalt porphyrin systems which undergoes rapid degenerative exchange when P_n-Mt^{x+1}/L finds itself in the presence of excess radicals.

Methyl acrylate was initially chosen as the common monomer, with the dormant chain modelled by the $CH_3(COOCH_3)CH^{\bullet}$ radical, namely replacing the polymer chain beyond the radical carrying chain-end unit with a hydrogen atom. This monomer choice does not appear the most appropriate one to probe the CCT activity of cobalt systems,

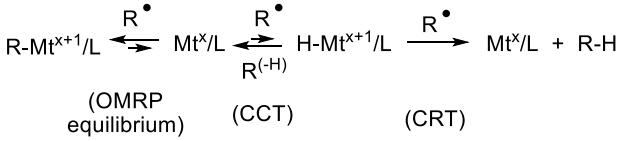

Scheme 3. Investigated reaction coordinate.

because acrylates are not the monomers leading most easily to CCT (relative to *e.g.* methacrylates and styrene).[18] This phenomenon is attributed to the stronger bond established between the acrylate radical and cobalt (OMRP dormant species), thus leaving a lower equilibrium amount of the Co^{II}/L catalyst to operate the CCT process. Indeed, a living chain growth controlled by the OMRP equilibrium is often observed for these monomers using cobalt complexes.[30, 31] On the other hand, acrylates are the monomers most readily involved in CRT with copper catalysts. It is important to compare the energy profile of the CCT and CRT for two representative metal complexes using the same radical species. Selected studies, however, were also carried out for the porphyrin system with the $(CH_3)_2(COOCH_3)C^{\bullet}$ radical as a model of the methyl methacrylate polymer chain, even though the reactivity of the isobutyrate radical is quite different from the PMMA radical, due to a strong penultimate effect.[32]

The two metal complexes were selected in order to be both representative and manageable in terms of computational time. The chosen cobalt system is [Co(porphyrin)] (**A** in Scheme 4), since porphyrinato derivatives of cobalt(II) are commonly used in radical polymerization.[30, 31, 33, 34] The most successful complexes, leading to OMRP with acrylate monomers and CCT for methacrylate monomers, contain substituents on the pyrrole C3 and C4 positions or on the methine bridges, such as for instance tetramesitylporphyrin (TMP). However, removing the ring substituents is not considered to introduce a strong electronic perturbation while greatly reducing the computational effort. The same simplification was adopted in previous computational studies of the [Co(porphyrin)] system.[35, 36] It should also be underlined that these previous studies have addressed the OMRP equilibrium[35] and the β-H atom transfer (CCT) equilibrium[36] for a different radical species ($CH_3(OAc)CH^{\bullet}$, modelling the PVAc growing radical chain), but did not investigate the CRT process. Selected calculations have also been carried out on the full (TMP)Co system using the QM/MM methodology, treating the four mesityl groups at the molecular mechanics level.

The selected copper system is $[Cu(TPMA)]^+$ (**B** in Scheme 4, TPMA = tris(2-pyridylmethyl)amine), since this complex gives CRT for methyl acrylate.[24] Thus, this calculation presents no simplifications of the real system. In addition, **B** is also a simplified model of the $[Cu(TPMA^*)]^+$ complex (TPMA* = tris((4-methoxy-3,5-dimethylpyridin-2-yl)methyl)amine), which also has CRT activity for methyl acrylate.[23]

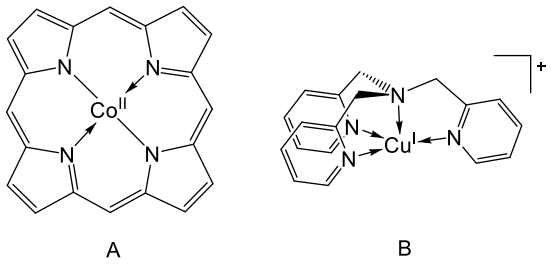

Scheme 4. Molecules used in this study.

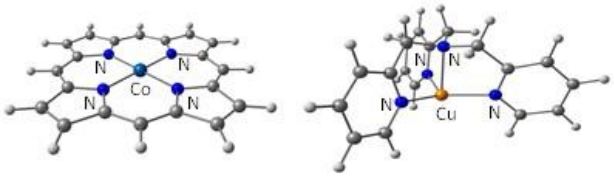

Figure 1. Optimized geometries of the $[Co^{II}(porphyrin)]$ (left) and $[Cu^{I}(TPMA)]^+$ (right) complexes.

All calculations were carried out using the BP86 functional, which was also employed in the already mentioned previous [Co(porphyrin)] computational study[35, 36] and found much more adapted than the more popular B3LYP functional. However, rather than adopting the same strategy of the previous study, which employed a low-quality basis set for optimizations followed by single point calculations with an improved basis set, we carried out optimizations directly with a high quality basis set constituted by 6-311G(d,p) functions for the light atoms (O,N,C,H) and LANL2DZ(f) for the metal atoms (Co, Cu). The electronic energy values were corrected for ZPVE, thermal (PV, TS), solvent and dispersion effects. Views and Cartesian coordinates for all optimized structures are available in the SI (Table S1).

(b) Optimized minima

The optimized geometries of the two Mt^x/L complexes are shown in Figure 1. The cobalt complex was optimized in the experimentally well-established doublet state,[37] whereas the copper complex is diamagnetic.

Addition of the $CH_3(COOCH_3)CH^{\bullet}$ ($R^{\bullet}$) radical leads to the formation of the OMRP dormant species, represented in Figure 2. The R-Co^{III} complex is diamagnetic, as well established for a number of 5-coordinate organocobalt(III) species, for instance Co(TMP)(CH_2tBu).[38] The geometry of the spin doublet R-Cu^{II} product is pseudo-trigonal bipyramidal, as observed for the related $[Cu(TPMA)X]^+$ complexes (X = Cl, Br;[39] no alkyl derivatives of this type have been isolated).

The calculated ΔG^0_{298} for the Co-R bond breaking process, with all corrections included, is 21.6 kcal/mol, whereas the value related to the Cu-R bond is much weaker, 14.5 kcal/mol, see Figure 3. The stronger bond calculated for the cobalt system is in line with the observed controlled polymerization of MA by [Co(porphyrin)] derivatives, whereas copper systems electronically related to $[Cu(TPMA)]^+$ do show a slowdown of

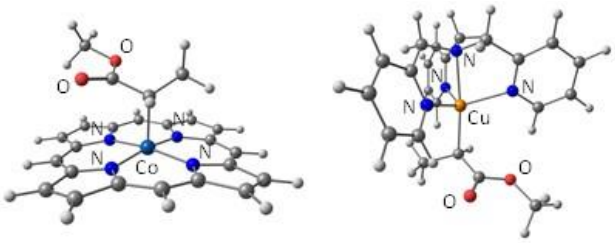

Figure 2. Optimized geometries of the OMRP dormant species $[R\text{-}Co^{III}(porphyrin)]$ (left) and $[R\text{-}Cu^{II}(TPMA)]^+$ (right), R = $CHCH_3(COOCH_3)$.

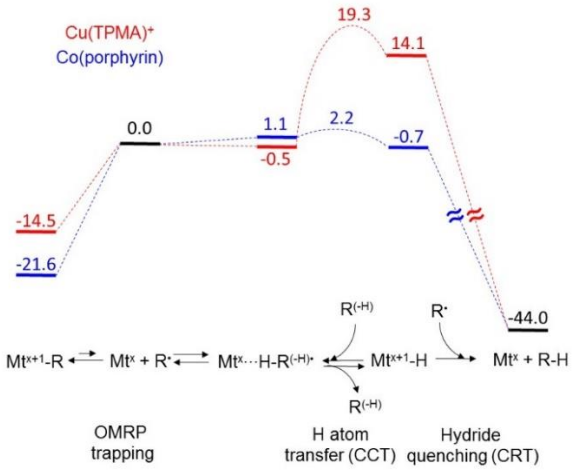

Figure 3. Gibbs energy profile (corrected for dispersion and solvation effects) for the investigated reactions. The relative G values are given in kcal/mol.

the MA polymerization but without a sufficient level of control.[23, 40]

From the computational point of view, it should be underlined that while the solvation correction makes a relatively small and weakening contribution to the homolytic bond strengths (-4.1 and -2.1 kcal/mol for the Co and Cu system, respectively), the dispersion interaction correction makes a very large strengthening contribution (+19.4 and +14.2 kcal/mol, respectively). The value calculated here for [(porphyrin)Co-$CH(CH_3)(COOCH_3)$] may be compared with 22.8 kcal/mol calculated using the same functional for the homolytic dissociation of [(porphyrin)Co-$CH(CH_3)(OCOCH_3)$], though without solvent or dispersion correction and for the gas phase standard state.[35] Given that these corrections have the overall effect of increasing the dissociation energy, the comparison is consistent with the notion that the more stabilized methyl acrylate-related $^{\bullet}CH(CH_3)(COOCH_3)$ radical forms weaker bonds than the vinyl acetate-related $^{\bullet}CH(CH_3)(OCOCH_3)$ radical.[41] The Co-C BDE was also calculated, at the same level of theory, for the $^{\bullet}C(CH_3)_2(COOCH_3)$ (methyl methacrylate-related) radical, yielding 14.8 kcal/mol when all corrections are included (dispersion and solvent PCM in MMA). This is much weaker than the bond to the methyl acrylate-related radical (21.6 kcal/mol), as expected.

The reaction coordinate that ultimately transfers the radical β-H atom to the metal atom starts with the establishment of a van der Waals [L/Mt^x···H-CH_2-$CH^{\bullet}$(COOMe)] adduct. The optimized geometry of this adduct gives a slightly higher Gibbs energy for the Co(porphyrin) system (1.1 kcal/mol relative to the two separate components). For the above mentioned related Co(porphyrin) + $^{\bullet}CH(CH_3(OAc)$ system,[36] a similar energy minimum was also optimized and found (ΔG = -2.66 kcal/mol relative to the separate species in the gas phase). Like for that system, this adduct gave a closed-shell singlet solution, even though the geometry was optimized as a broken symmetry open-shell singlet. This shows that complete quenching of the two radicals spin density has already taken place at the level of this adduct. The C-H and H-Co distances, highlighted in the

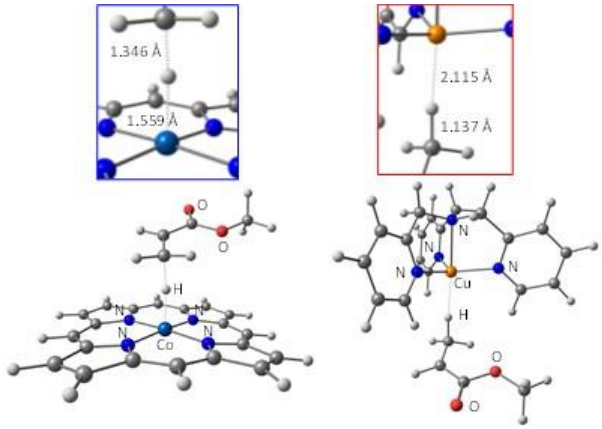

Figure 4. Optimized geometries of the van der Waals [L/Mt^x···H-CH_2-$CH^{\bullet}$(COOMe)] adduct [L/Mt^x = Co^{II}(porphyrin), left; Cu^{II}(TPMA)$^+$, right].

detailed image of Figure 4 (left), illustrate that extensive C-H bond stretching has taken place and that the H-Co separation is already rather close to that of the final hydride product (*vide infra*). The corresponding optimized van der Waals adduct for the Cu system, on the other hand, exhibits a rather loose interaction between the C-H bond, which is only slightly elongated relative to the other C-H bonds (see excerpt in Figure 4, right), and the copper atom. The energy is essentially unchanged relative to the sum of the two separate species (-0.5 kcal/mol), even less so than for the Co(porphyrin system). The spin density in this adduct is almost entirely localized on the organic fragment (0.809 on the C atom and 0.163 on the carbonyl O atom) with only 0.04 being transferred to the Cu atom.

The product of the β-H atom transfer to Mt^x/L, namely the hydride complex H-Mt^{x+1}/L, has the same basic geometry of the OMRP dormant species, see Figure 5. The optimized Mt^{x+1}-H distances are 1.412 Å for the Co^{III} system and 1.551 Å for the Cu system. Relative to the Mt^x/L precursor, the hydride systems are less stabilized than OMRP species. This is because whereas the OMRP species is generated by a simple Mt-C bond formation process, formation of the Mt-H bond in the examined process is accompanied by the bond breaking of a strong C-H bond, which is partially compensated only by the formation of a weaker C-C π bond. Like for the generation of the OMRP species, the process is less energetically favourable for the [Cu(TPMA)]$^+$ system than for the [Co(porphyrin)] system, see Figure 3. There is a greater difference in favour of the cobalt system for the CCT process (14.8 kcal/mol) than for the OMRP trapping process (7.1 kcal/mol). The most relevant consequence of this phenomenon is that the H atom transfer process is close

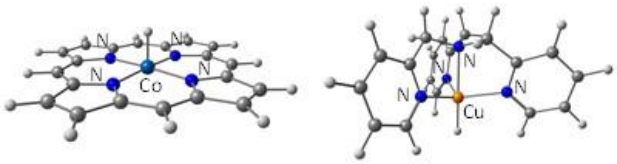

Figure 5. Optimized geometries of the CCT/CRT hydride intermediate complex, [H-Co^{III}(porphyrin)] (left) and [H-Cu^{II}(TPMA)]$^+$ (right).

to thermoneutral for the [Co(porphyrin)] system while it is significantly endothermic for the copper system. In the previous study of the β-H atom transfer process to [Co(porphyrin)] the reaction was also calculated as exothermic (-5.1 kcal/mol from the $^{\bullet}C(CH_3)_2(CN)$ radical and -13.6 kcal/mol from the $^{\bullet}CH(CH_3)(OCOCH_3)$ radical).[36] In this case, both solvation (-1.7 kcal/mol) and dispersion (+0.2 kcal/mol) effects are very small since the process involves two molecules on each side.

(c) CCT transition state

The optimized transition state of the β-H atom transfer process is represented in Figure 6. The H-atom transfer for the [Co(porphyrin)] system occurs smoothly, with an activation barrier of only 2.2 kcal/mol on the G scale for the forward process (generation of the hydride intermediate) and 2.9 kcal/mol for the backward process. As also previously found for the corresponding calculation on the Co(porphyrin)/$^{\bullet}CH(CH_3)(OAc)$ system[36] and by analogy to the van der Waals minimum described above, the broken symmetry open-shell minimum optimization led to a closed-shell singlet solution, with a spin density of essentially zero on every atom. Compared to the optimized geometry of the van der Waals adduct, the C-H bond is further stretched and the Co-H bond is almost fully formed (see the close-up image of Figure 6, left) but the changes are minimal. The β-H atom transfer transition state leading to the (porphyrin)Co-H intermediate was also optimized when involving the methacrylate related radical $^{\bullet}C(CH_3)_2(COOCH_3)$, yielding an even lower barrier (0.3 kcal/mol). This agrees with the great propensity of methyl methacrylate to undergo CCT.

On the other hand, the barrier is much greater for the $[Cu(TPMA)]^+$ system, in the forward direction (19.3 kcal/mol, in part because of the endothermic transformation) but also in the backward direction (5.2 kcal/mol). This means that the $[H\text{-}Cu(TPMA)]^+$ intermediate is slower in transferring back the H atom to a new monomer relative to the [H-Co(porphyrin)] intermediate. The bonding details of the C···H···Mt moiety in the transition state indicate a slightly longer Cu···H separation (see the close-up image of Figure 6, right). The Mt-H bond lengthening on going from the hydride complex to the transition state is actually greater for the cobalt system (Δd = 0.069 Å) than for the copper system (Δd = 0.038 Å). However, this bond lengthening is compensated by a much greater degree of C-H bond forming in the cobalt case (C···H = 1.596 Å) than for the copper case (C···H = 1.959 Å, *vs.* a C-H bond distance of 1.107 Å in the radical product). The spin density related to the single unpaired electron in the copper system is delocalized essentially on the Cu centre (0.383), on the transferring H atom (0.283) and on the α-C atom that eventually carries the spin density in the radical product (0.223).

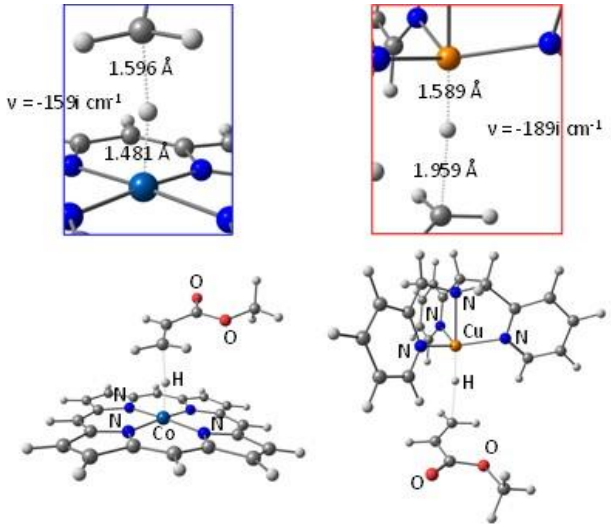

Figure 6. Optimized geometries of the β-H atom transfer transition state and close-up of the C···H···Mt moiety for the [Co(porphyrin)] (left) and $[Cu(TPMA)]^+$ (right) systems.

(d) Hydride quenching along the CRT pathway

One possible hypothesis to rationalize the preference of the cobalt system for H atom transfer to olefin (monomer) rather than to radical is to imagine that the latter process involves a greater barrier, while the opposite preference (greater barrier to transfer to monomer than to radical) would occur for the copper hydride intermediate. However, a partial optimization scan for the two systems indicates that the H atom transfer to radical is electronically barrierless in both cases (Figure 7). It is interesting to note that the hydride-radical interaction develops at an earlier stage along the transfer coordinate for the copper system, a significant energy gain being already evident at a C···H distance > 2 Å (e.g. 7.8 kcal/mol at 2.44 Å and 23.7 kcal/mol at 1.94 Å). For the cobalt system, on the other hand, the energy is lowered by < 4 kcal/mol at a distance of 2 Å.

For the cobalt system, the global spin state along this specific reaction coordinate is ½, with the unpaired spin being transferred from the free radical, which becomes the diamagnetic alkane product, to the diamagnetic hydride complex, which regenerates the spin doublet [Co(porphyrin)] catalyst. A Mulliken analysis shows the gradual transfer of the spin density from the C atom (for the hydride + radical combination at long C···H distances) to the cobalt atom (for the catalyst + alkane combination at short C···H distances).

For the copper system, the spin state is also invariable from beginning to end: spin zero for the antiferromagnetic

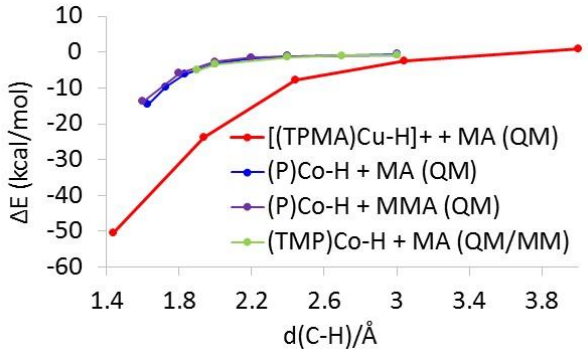

Figure 7. Energy profile for the H atom transfer from the different $H\text{-}Mt^{x+1}/L$ systems to the $^{\bullet}CH(CH_3)(COOCH_3)$ radical (red, blue and green lines) or to the $^{\bullet}C(CH_3)_2(COOCH_3)$ radical (purple line).

combination the spin doublet hydride and organic radical on one side and for the copper(I) catalyst and alkane products on the other side. However, the antiferromagnetic combination of the two radicals required the entire scan to be explored in broken symmetry. Indeed, the restricted spin zero calculations for long C···H distances only yielded charge transfer excited states. At infinite distance, the hydride complex has the majority of the spin density on the Cu atom (-0.691) and on the hydridic H atom (-0.291) whereas the radical has the majority of the spin density on the C atom (+0.858), the rest being delocalized on the carboxylic function. When the two species are still quite separated from each other (C···H = 3.04 Å), the spin density is already significantly decreased (Cu, -0.393; H, -0.283; C, +0.717). At a C···H distance of 2.44 Å, all the spin density is already completely quenched with < 0.001 remaining on the Cu and the C atoms.

Figure 8 shows the geometries of the two systems at approximately the same C···H distance. The Mt-H bond lengthening relative to the optimized hydride complex is quite comparable for the two metal systems (Co: 1.470 Å, Δ = +0.058 Å; Cu: 1.612 Å, Δ = +0.061 Å), although the energetic stabilization is quite different has shown in Figure 7. This is likely related to the spin density quenching process.

The hydride quenching for the Co(porphyrin) model was also explored with the $^{\bullet}C(CH_3)_2(COOCH_3)$ radical, a model of the methyl methacrylate growing chain for which the highest CCT activity is experimentally observed for this catalyst family. No CRT has so far been reported for Co(porphyrin)-type CCT catalysts. It is therefore of interest to probe whether the introduction of a second methyl group on the radical carrying C atom would introduce a sterically related barrier, hampering the H atom transfer to radical. However, as shown in Figure 7, the energy profile for the Co(porphyrin)/$^{\bullet}C(CH_3)_2(COOCH_3)$ system is essentially identical to that of the Co(porphyrin)/$^{\bullet}CH(CH_3)(COOCH_3)$ system. At a C-H distance of 2.0 Å (see view in Figure 9), the Co-H bond lengthening is identical to that observed for the acrylate-related radical (1.470 Å, Δ = +0.058 Å).

Finally, wondering whether the lack of CRT could be related to the steric impediment of the porphyrin ring substituents, we have carried out calculations of the CRT hydride quenching step for the full (TMP)Co-H molecule. Given the considerable size of the molecule, the four mesityl substituents were handled at the molecular mechanics level in a QM/MM approach. This methodology is nevertheless able to capture any existing steric

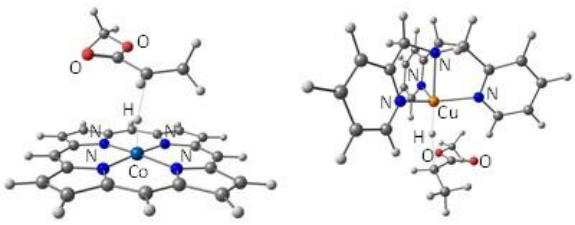

Figure 8. Partially optimized geometries (fixed C···H distance) along the H atom transfer from the H-Mt^{x+1}/L intermediate to the $^{\bullet}CH(CH_3(COOCH_3)$ radical. Left: [Co(porphyrin)] system (C···H = 2 Å); right: [Cu(TPMA)]$^{+}$ system (C···H = 1.94 Å).

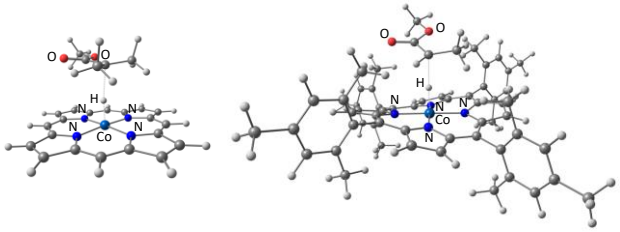

Figure 9. Partially optimized geometries (fixed C···H distance of 2.0 Å) along the H atom transfer from the H-Co(porphyrin) intermediate to the $^{\bullet}C(CH_3)_2(COOCH_3)$ radical at the full QM level (left) and from the H-Co(TMP) intermediate to the $^{\bullet}CH(CH_3)(COOCH_3)$ radical at the QM/MM level (right).

effect. The results of the calculations, also shown in Figure 7, indicate however that the energy curve follows exactly the same trends of the $^{\bullet}CH(CH_3)(COOCH_3)$ and $^{\bullet}C(CH_3)_2(COOCH_3)$ radical approaches to the simplified Co(porphyrin) model. For the fixed C-H distance of 2.0 Å (Figure 9), the Co-H bond lengthening is only marginally smaller (1.467 Å, Δ = +0.055 Å) than those of the acrylate and methacrylate related radicals at the same C-H distance. This indicates that four mesityl groups do not introduce a significant steric effect on the putative hydride quenching pathway. The introduction of the mesityl groups imposes a slight corrugation of the porphyrin ring, which is found also in the fully optimized (TMP)Co^{III}(H) molecule and is essentially independent on the C-H distance along the CRT hydride quenching pathway.

Discussion

Comparison of the OMRP/CCT/CRT energy profiles involving either the [Co(porphyrin)] or the [Cu(TPMA)]$^{+}$ systems (Figure 3) is not sufficient to fully rationalize their different behaviour under OMRP conditions. In particular, it is well known that [Co(porphyrin)]-type systems are efficient chain transfer catalysts under conditions where the hydride intermediate is in the simultaneous presence of monomer and radicals and a CRT phenomenon has not yet been reported for this metal. The profile in Figure 7, however, suggests that once the hydride complex is generated, its quenching by an additional radical should occur very favourably to yield a CRT process, even though the H transfer to monomer to complete the CCT cycle is also facile. The analysis of the same quenching pathway upon introduction of steric bulk in the radical (*e.g.* going from the acrylate to the methacrylate related radical) or in the porphyrin ring (going to the real TMP ligand) do not significantly alter the CRT hydride quenching pathway and notably do not introduce a sterically related electronic barrier. The only expected free energy barrier is entropic, mostly related to the loss of translational and rotational degrees of freedom upon association of the two separate partners and is therefore expected to be substantially similar for all investigated systems (Figure 7).

However, there is a kinetic factor to be kept in mind. The two competitive processes that lead to consumption of the hydride intermediate should follow the rate laws:

transfer to olefin (CCT): k_{CCT}[H-Mt^{x+1}/L][R$^{(\cdot H)}$]; (1)

transfer to radical (CRT): k_{CRT}[H-Mt^{x+1}/L][R$^{\bullet}$]. (2)

Although the activation barriers may be in favour of the CRT process (k_{CRT} > k_{CCT}), at least for the copper system, the concentrations are very much in favour of CCT ([R$^{(-H)}$] >> [R$^{\bullet}$]). Considering that the CCT barrier is quite small for the cobalt system and should be even less effected by steric encumbrance in the porphyrin ring and in the radical relative to the CRT barrier (the H atom transfer involves a more accessible sp^2 C atom in the monomer), the efficiency of the cobalt system as a chain transfer catalyst appears qualitatively rationalized.

We also have to take into consideration that a minor contamination of the CCT activity with a catalysed termination would remain undetected, because the $P_n^{(-H)}$ chains (unsaturated chain ends) generated by disproportionation are common to the CCT process and the $P_n^{(H)}$ chains (saturated chain ends) may also be generated by the spontaneous (non-catalysed) radical terminations. Hence, it is quite possible that the CRT process indeed occurs also for cobalt systems, but only to a small extent not allowing its clear identification.

Moving now to the more challenging copper system, the energetic profile in Figure 3 shows that generation of the hydride intermediate is slower. More importantly, there is a greater barrier for H atom transfer to olefin, hence this process should also be slower. On the other hand, Figure 7 indicates that H atom transfer to the radical, like for the cobalt system, does not have any barrier and the stabilizing effect develops at greater C···H distances. Therefore, in the comparative rate expressions for the consumption of the hydride intermediate (equations 1 and 2), the k_{CRT}/k_{CCT} ratio is expected to be much greater in the copper system. In addition, because of the ligand structure and coordination geometry, steric effects in the ligand system are less likely to perturb the CRT pathway and therefore to disfavour it relative to CCT. This is because the H atom is relatively accessible in the trigonal bipyramidal geometry of the [H-Cu^{II}(TPMA)]$^+$ complex (see Figure 8) and substitution on the pyridine rings at the 3, 4 and 5 positions in the TPMA* system does not affect the open space around the hydride ligand.

On the basis of these considerations, we may argue on what kind of ligand engineering might allow reducing the impact of CRT in either an ATRP or OMRP process. In ATRP, the dominant metal species is generally the copper(I) complex, unless the redox properties and reactivity of the complex and/or the nature of the polymerized monomer favour the establishment of a strong Cu^{II}-R bond. For instance, in the [Cu(TPMA)]$^+$/MA system, analysed in this contribution, the formation of the OMRP dormant species appears favourable (Figure 3), but the halogen atom transfer also becomes more favoured for very active ATRP catalysts and the dominant species in the system may in fact become a Br-Cu^{II} species.[42, 43] Thus, the concentration of CRT catalyst is generally high. One solution to this problem has already been highlighted:[24] while the CRT activity depends on the [Cu^{I}] concentration (to which the [H-Cu^{II}] concentration in equation 2 is proportional), the overall rate of ATRP depends on the [Cu^{I}/L]/[X-Cu^{II}/L] ratio, thus lowering the overall catalyst concentration while maintaining the same ratio of reduced and oxidized forms, as in the ARGET-ATRP protocol,[24, 44-46] allows maintaining a high polymerization rate while decreasing the impact of CRT. In order to further diminish the CRT process, it is necessary to disfavour the formation of the hydride intermediate and especially of the transition state leading to it. Once the hydride intermediate is formed, it may be difficult or impossible to manipulate the ligand coordination sphere in order to force the system to transfer the H atom to monomer (CCT activity) rather than to radical.

Concerning OMRP, copper has so far not shown any useful applications, contrary to cobalt. This also contrasts with the ubiquitous role of copper in ATRP. Early studies have shown that a copper complex, [Cu(R-bipy)$_2$]$^+$ (R-bipy = substituted bipyridine), slows down the polymerization of acrylates but does not insure any reasonable level of control.[40] The same occurs for [Cu(TPMA)]$^+$ and [Cu(TPMA*)]$^+$.[23, 24] Hence, the Cu^{I} catalyst concentration remains relatively high and extensive CRT can take place under these conditions. The reasonable question to ask is whether OMRP with Cu complexes has a potential under any circumstances. The attempts to use copper complexes under OMRP conditions have so far been limited to reactive monomers (such as acrylates, styrene). Less reactive monomers (e.g. vinyl acetate) should lead to stronger Cu^{II}-C bonds in the OMRP dormant species,[11] thus the OMRP equilibrium should contribute to lowering the CRT catalyst concentration. Under these conditions, if the activation barrier for the β-H atom transfer leading to the formation of the hydride intermediate remains high, the impact of CRT should decrease and developing a Cu-based OMRP with reasonable control should become possible.

Conclusions

The present DFT study has provided a framework of understanding for the contrasting behaviour of cobalt(II) and copper(I) systems in terms of their catalytic activity, under essentially identical experimental conditions, in competing chain transfer and radical termination processes. For both systems, the two catalytic processes occur via the same hydride species, Co^{III}-H or Cu^{II}-H respectively. In terms of electronic energy, the hydride quenching by radical leading to CRT is barrierless for both systems, although the associative nature of the reaction introduces an entropy related barrier. A significant interaction starts to develop at longer H···C distances for the copper system because of the spin density quenching between the two radical species. On the other hand, the H transfer to monomer has a relatively high electronic barrier for the Cu system and thus CRT prevails, although the much greater monomer concentration should favour CCT. Conversely, the cobalt system features a low energy hydride intermediate and a very low electronic barrier for H atom transfer to monomer. This is related to the spin quenching process along the conversion of the (porphyrin)Co^{II}/organic radical pair to the combination of hydride and olefin. In combination with the dominant monomer concentration, the resulting energy profile favour CCT activity. The acquired understanding illustrates the necessary conditions for limiting the CRT phenomenon in the

application of copper complexes in ATRP and also in the OMRP of less reactive monomers.

Acknowledgements

We thank the CNRS (Centre National de la Recherche Scientifique) for support of this work through the PICS 06782 grant. RP also acknowledges additional support from ANR (Agence National de la Recherche) through the project FLUPOL (grant ANR-14-CE07-0012) and KM acknowledges additional support from the NSF (DMR 1400052). This work was granted access to the HPC resources of CINES and IDRIS under the allocation (2006 through 2015)-086343 made by GENCI (Grand Equipement National de Calcul Intensif) and to the resources of the CICT (Centre Interuniversitaire de Calcul de Toulouse, project CALMIP).

References

1. A. D. Jenkins, R. G. Jones and G. Moad, *Pure Appl. Chem.*, 2010, **82**, 483-491.
2. K. Matyjaszewski, Y. Gnanou and L. Leibler, *Macromolecular Engineering: Precise Synthesis, Materials Properties, Applications*, Wiley-VCH Verlag GmbH, 2007.
3. K. Matyjaszewski and J. H. Xia, *Chem. Rev.*, 2001, **101**, 2921-2990.
4. M. Kamigaito, T. Ando and M. Sawamoto, *Chem. Rev.*, 2001, **101**, 3689-3745.
5. N. V. Tsarevsky and K. Matyjaszewski, *Chem. Rev.*, 2007, **107**, 2270-2299.
6. W. A. Braunecker and K. Matyjaszewski, *Progr. Polym. Sci.*, 2007, **32**, 93-146.
7. M. Ouchi, T. Terashima and M. Sawamoto, *Chem. Rev.*, 2009, **109**, 4963-5050.
8. R. Poli, *Eur. J. Inorg. Chem.*, 2011, 1513-1530.
9. R. Poli, *Angew. Chem. Int. Ed. Engl.*, 2006, **45**, 5058–5070.
10. R. Poli, in *Polymer Science: A Comprehensive Reference*, eds. K. Matyjaszewski and M. Möller, Elsevier BV, Amsterdam, 2012, vol. 3, pp. 351–375.
11. R. Poli, *Chem. Eur. J.*, 2015, **21**, 6988-7001.
12. K. M. Smith, W. S. McNeil and A. S. Abd-El-Aziz, *Macromol. Chem. Phys.*, 2010, **211**, 10-16.
13. M. Hurtgen, C. Detrembleur, C. Jerome and A. Debuigne, *Polym. Rev.*, 2011, **51**, 188-213.
14. L. E. N. Allan, M. R. Perry and M. P. Shaver, *Progr. Polym. Sci.*, 2012, **37**, 127-156.
15. K. Matyjaszewski, *Macromol. Symp.*, 1998, **134**, 105-118.
16. K. Matyjaszewski, K. Davis, T. E. Patten and M. Wei, *Tetrahedron*, 1997, **53**, 15321-15329.
17. K. Matyjaszewski, N. V. Tsarevsky, W. A. Braunecker, H. Dong, J. Huang, W. Jakubowski, Y. Kwak, R. Nicolay, W. Tang and J. A. Yoon, *Macromolecules*, 2007, **40**, 7795-7806.
18. A. A. Gridnev and S. D. Ittel, *Chem. Rev.*, 2001, **101**, 3611-3659.
19. J. P. Collman, L. S. Hegedus, J. R. Norton and R. G. Finke, *Principles and Applications of Organotransition Metal Chemistry*, University Science Books, Mill Valley, CA, 1987.
20. Z. Lu, M. Fryd and B. B. Wayland, *Macromolecules*, 2004, **37**, 2686-2687.
21. B. B. Wayland, C.-H. Peng, X. Fu, Z. Lu and M. Fryd, *Macromolecules*, 2006, **39**, 8219-8222.
22. C. H. Peng, J. Scricco, S. Li, M. Fryd and B. B. Wayland, *Macromolecules*, 2008, **41**, 2368-2373.
23. K. Schröder, D. Konkolewicz, R. Poli and K. Matyjaszewski, *Organometallics*, 2012, **31**, 7994-7999.
24. Y. Wang, N. Soerensen, M. Zhong, H. Schroeder, M. Buback and K. Matyjaszewski, *Macromolecules*, 2013, **46**, 683-691.
25. H. Schroeder and M. Buback, *Macromolecules*, 2014, **47**, 6645-6651.
26. G. Moad and D. H. Solomon, *The Chemistry of free Radical Polymerization*, Elsevier, Amsterdam, 2nd edn., 2006.
27. M. P. Shaver, L. E. N. Allan, H. S. Rzepa and V. C. Gibson, *Angew. Chem. Int. Ed. Eng.*, 2006, **45**, 1241-1244.
28. L. E. N. Allan, M. P. Shaver, A. J. P. White and V. C. Gibson, *Inorg. Chem.*, 2007, **46**, 8963-8970.
29. R. Poli and M. P. Shaver, *Chem. Eur. J.*, 2014, **20**, 17530–17540.
30. B. B. Wayland, L. Basickes, S. Mukerjee, M. Wei and M. Fryd, *Macromolecules*, 1997, **30**, 8109 - 8112.
31. A. Debuigne, R. Poli, C. Jérôme, R. Jérome and C. Detrembleur, *Prog. Polym. Sci.*, 2009, **34**, 211-239.
32. C. Y. Lin, M. L. Coote, A. Petit, P. Richard, R. Poli and K. Matyjaszewski, *Macromolecules*, 2007, **40**, 5985-5994.
33. A. A. Gridnev, S. D. Ittel, M. Fryd and B. B. Wayland, *Organometallics*, 1996, **15**, 222-235.
34. A. A. Gridnev, S. D. Ittel, B. B. Wayland and M. Fryd, *Organometallics*, 1996, **15**, 5116-5126.
35. S. Li, B. de Bruin, C. H. Peng, M. Fryd and B. B. Wayland, *J. Am. Chem. Soc.*, 2008, **130**, 13373-13381.
36. B. de Bruin, W. I. Dzik, S. Li and B. B. Wayland, *Chem. Eur. J.*, 2009, **15**, 4312-4320.
37. B. B. Wayland and D. Mohajer, *J. Am. Chem. Soc.*, 1971, **93**, 5295-&.
38. H. Ogoshi, E. Watanabe, N. Koketsu and Z. Yoshida, *Bull. Chem. Soc. Jpn.*, 1976, **49**, 2529-2536.
39. W. T. Eckenhoff and T. Pintauer, *Inorg. Chem.*, 2010, **49**, 10617-10626.
40. K. Matyjaszewski and B. E. Woodworth, *Macromolecules*, 1998, **31**, 4718-4723.
41. M. B. Gillies, K. Matyjaszewski, P.-O. Norrby, T. Pintauer, R. Poli and P. Richard, *Macromolecules*, 2003, **36**, 8551-8559.
42. W. Tang, Y. Kwak, W. Braunecker, N. V. Tsarevsky, M. L. Coote and K. Matyjaszewski, *J. Am. Chem. Soc.*, 2008, **130**, 10702-10713.
43. N. Bortolamei, A. A. Isse, V. B. Di Marco, A. Gennaro and K. Matyjaszewski, *Macromolecules*, 2010, **43**, 9257-9267.
44. K. Min, H. F. Gao and K. Matyjaszewski, *Macromolecules*, 2007, **40**, 1789-1791.
45. K. Matyjaszewski, W. Jakubowski, K. Min, W. Tang, J. Y. Huang, W. A. Braunecker and N. V. Tsarevsky, *Proc. Nat. Acad. Sci.*, 2006, **103**, 15309-15314.
46. D. Konkolewicz, Y. Wang, M. J. Zhong, P. Krys, A. A. Isse, A. Gennaro and K. Matyjaszewski, *Macromolecules*, 2013, **46**, 8749-8772.